Supplementary data

Features		Frequency n (%)
Age (yrs)	Mean (range)	70 (36-96)
Tumor diameter (mm)	Mean (range)	49.1 (4-170)
Gender	Female	614 (51.9)
	Male	570 (84.1)
Tumor location	Left-sided	763 (65.2)
	Right-sided	407 (34.8)
Histologic subtype	Mucinous	97 (8.2)
	Non-mucinous	1088 (91.8)
pT stage	pT1-2	230 (19.8)
	pT3-4	932 (80.2)
pN stage	pN0	608 (53.4)
	pN1-2	531 (46.6)
Tumor grade	G1-2	1005 (86.6)
	G3	155 (13.4)
Vascular invasion	Absent	848 (73.1)
	Present	312 (26.9)
Mismatch repair status	Proficient	990 (83.5)
	Deficient	195 (16.5)
Local recurrence	Absent	262 (58.7)
	Present	184 (41.3)
Distant metastasis	Absent	370 (81.9)
	Present	82 (18.1)
Post-operative therapy	None	355 (79.4)
	Treated	92 (20.6)
Survival rate	5 year (95%CI)	57.4 (54-60)

Table S1: Patient characteristics (n=1185).

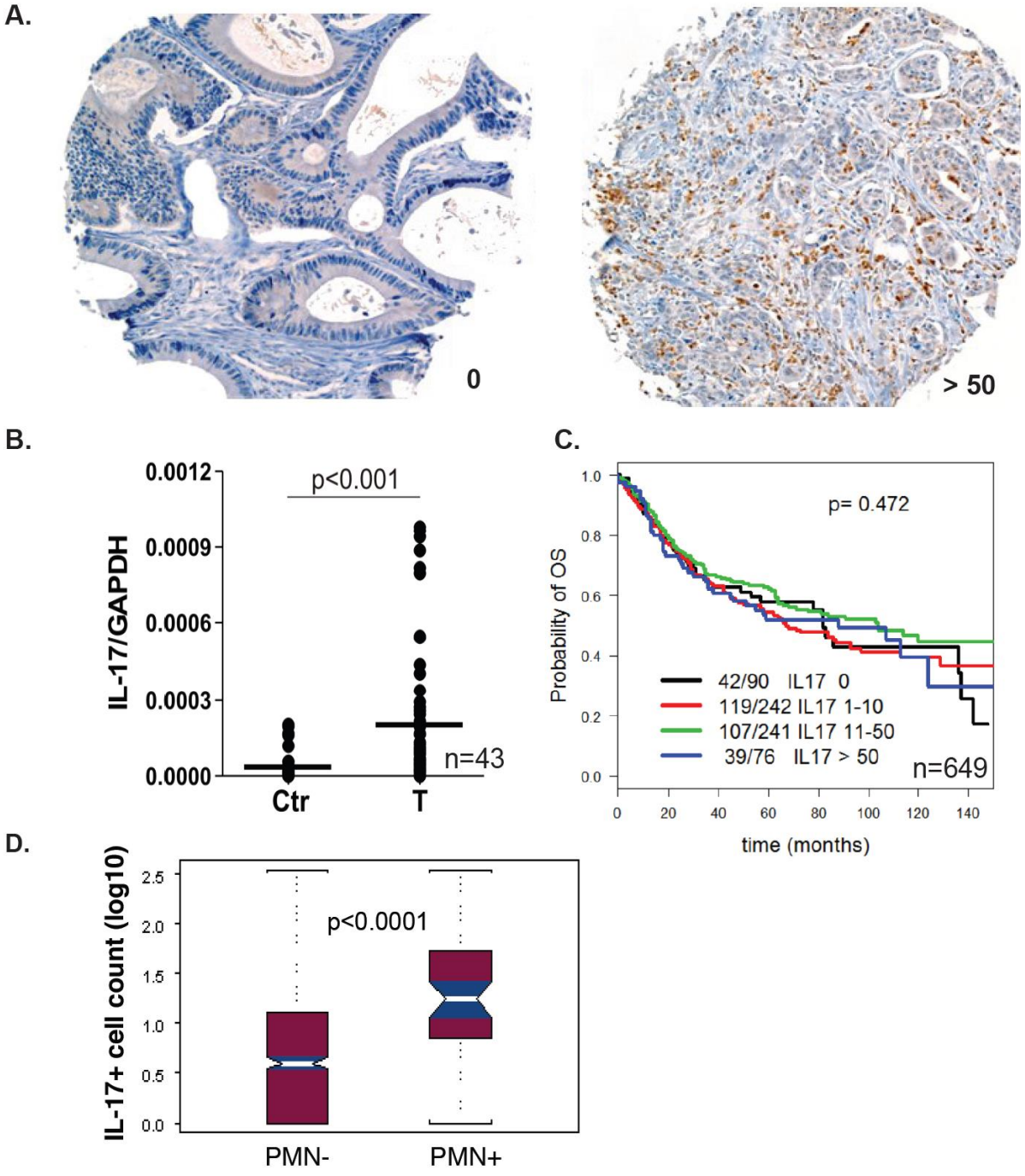

Figure S1. Prevalence and prognostic significance of IL-17+ cells. IL-17 expression was evaluated by IHC on a randomized subgroup of cases, including 746 CRC and 27 healthy mucosa cases, with a rabbit polyclonal anti-human IL-17 (H-132, Santa Cruz Biotechnology, referred to as staining II). **A.** Representative pictures of staining II and numbers of IL-17+ cells per punch are shown. **B**. IL-17 mRNA levels assessed by quantitative PCR in tumor-free colonic mucosa (Ctr) and CRC (T) samples (n=43). **C.** Kaplan-Meyer curves illustrating overall survival (OS) probability according to IL-17+ cell density. Numbers of deaths/total cases (n=649) within each category are indicated. **D.** Association between numbers of IL-17+ cells in CRC cases characterized by absence or presence of infiltrating polymorphonuclear cells (PMN- and PMN+, respectively), as assessed upon H&E staining. Statistical significance was assessed by log rank test.

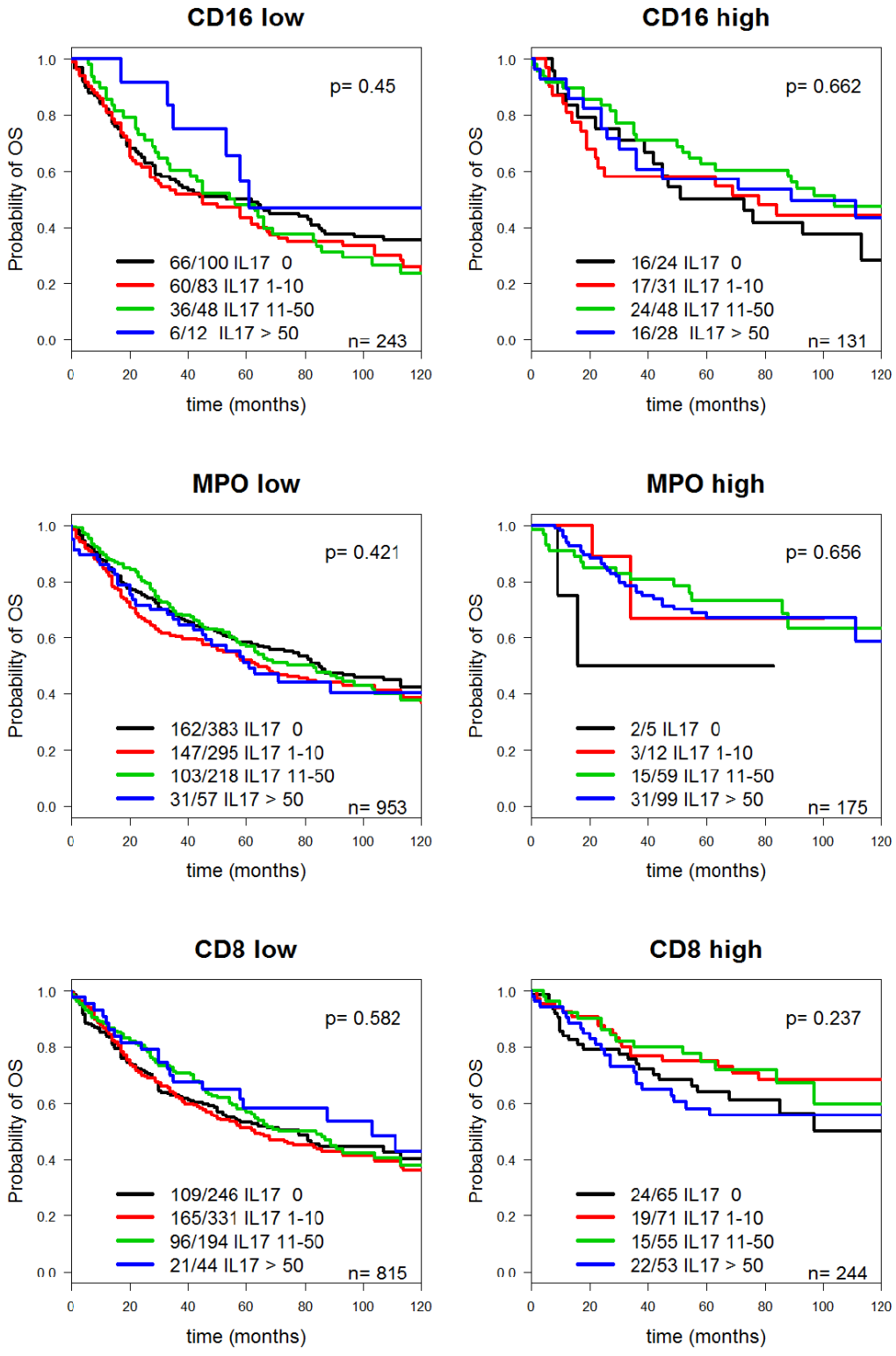

Figure S2. Clinical impact of IL-17+ cells on CRC infiltration by CD16+, MPO+, or CD8+ cells. Kaplan-Meyer curves illustrating overall survival (OS) probability according to IL-17+ cell density in CRC cases characterized by low or high infiltration by CD16+ , MPO +, or CD8+ cells. Numbers of deaths/total cases within each category are indicated. Statistical significance was assessed by log rank test.

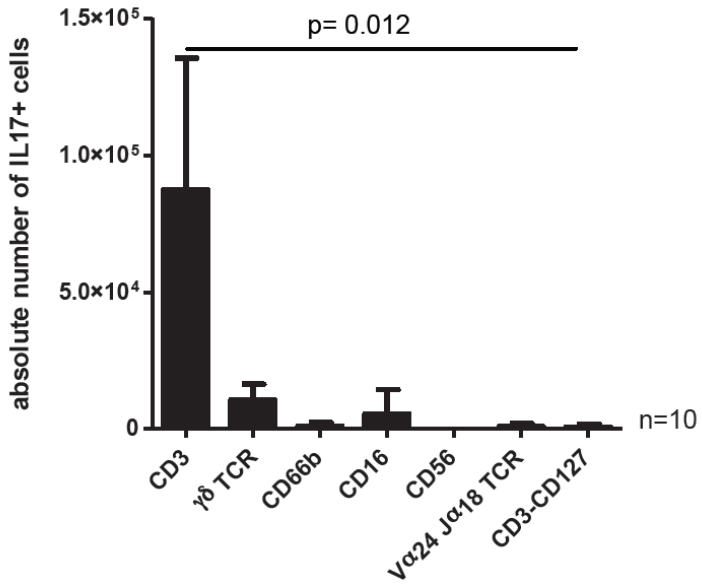

Figure S3. CRC-infiltrating IL-17+ cells mostly consist of Th17 cells. Absolute numbers of IL-17+ cells expressing the indicated markers, as assessed by flow cytometry on single cell suspensions obtained from CRC specimens (n=10).

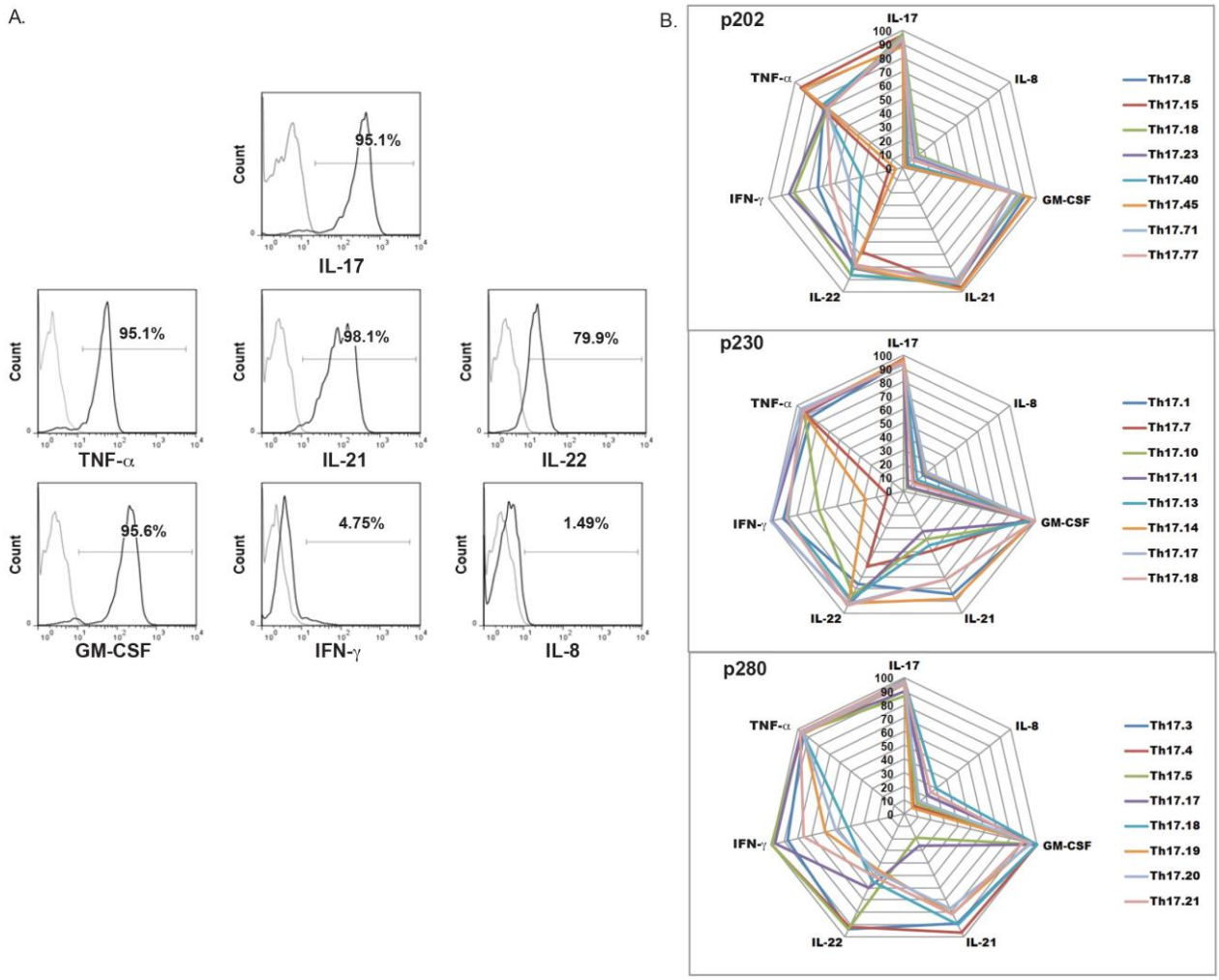

Figure S4. Cytokine production capacity of CRC-derived Th17 clones. A. Representative flow cytometric analysis of a CRC-derived Th17 clone. Cells were stimulated with PMA/Ionomycin/Brefeldin for 5 hours and intracellular staining was then performed. Staining with cytokine-specific antibodies (black histograms) or matched isotype controls (grey histograms) is shown. Frequencies of positive cells are indicated. **B.** Cytokine profiles of Th17 clones derived from 3 different patients. Percentages of cells positive for the indicated cytokines are depicted.

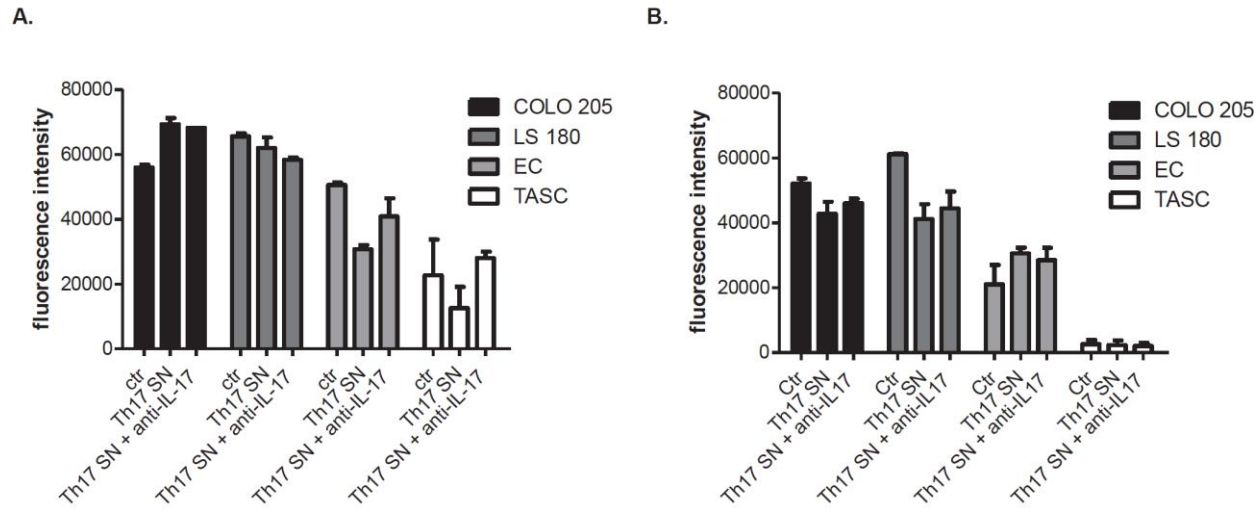

Figure S5. Proliferation of CRC, endothelial, and tumor-associated stromal cells cultured in the presence of CRC-Th17 supernatants. CRC cell lines (COLO 205 and LS 180), endothelial cells (EC), and tumor associated stromal cells (TASC) were cultured for 48h in the presence of Th17 supernatants derived from 3 clones from one sample (**A.**) and 3 bulk cultures from 3 samples (**B.**), untreated (Th17 SN) or pre-treated with anti-IL-17 neutralizing antibodies (Th17 + anti-IL-17). Cells proliferation was measured by CyQUANT assay.

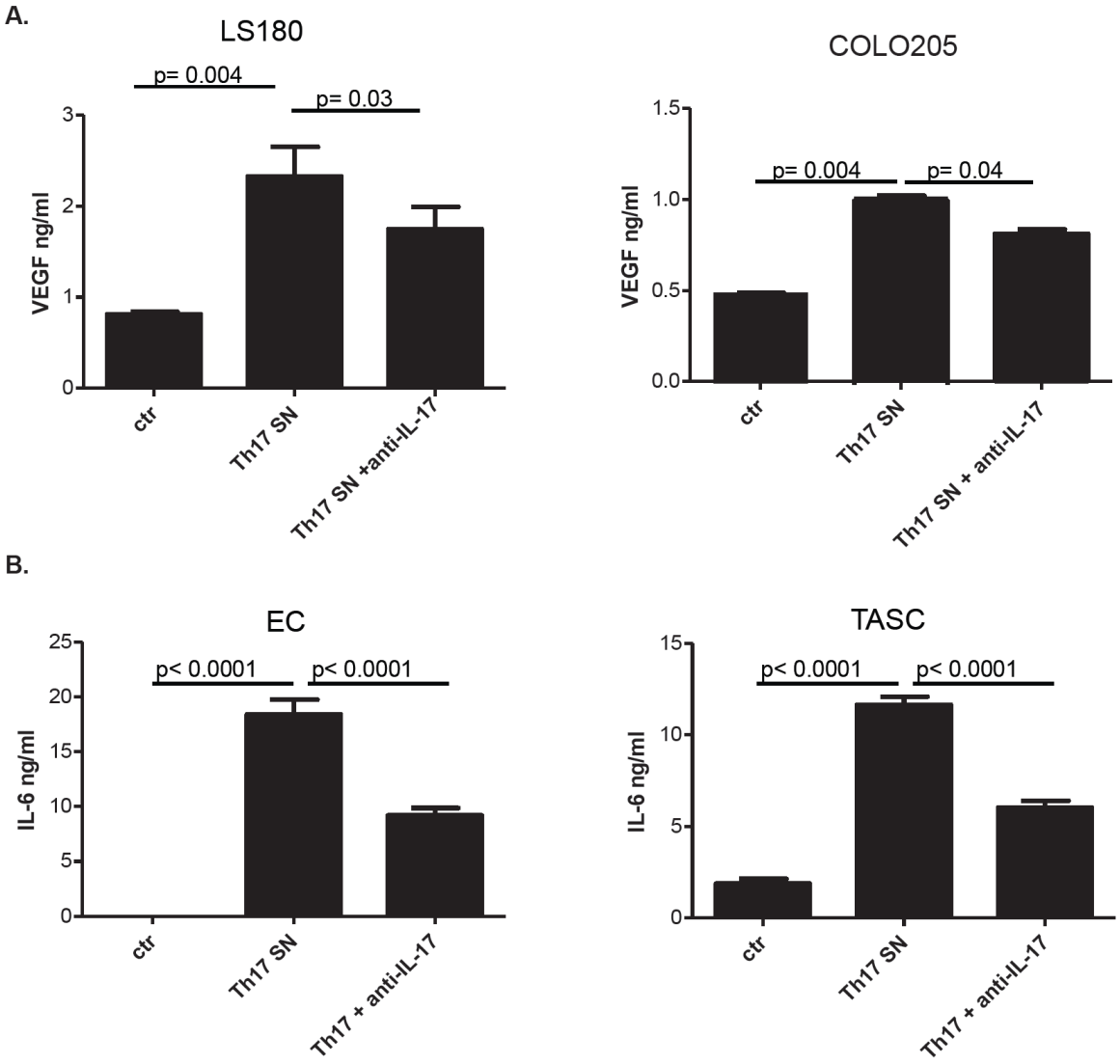

Figure S6. CRC-Th17 mediate protumorigenic effects in an IL-17-dependent manner. Endothelial (EC), tumor associated stromal cells (TASC), and CRC cell lines (LS180, COLO205), were conditioned for 24h with CRC-Th17 supernatants obtained from Th17 bulk populations, untreated (Th17 SN) or pre-treated with anti-IL-17 neutralizing antibodies (Th17 + anti-IL-17). VEGF (A) or IL-6 (B) release was measured in culture supernatants by ELISA. Statistical significance was analyzed by one-way ANOVA test. Data shown refer to experimental triplicates from 3 independent experiments performed with supernatants from Th17 bulk cultures derived from 3 different samples.

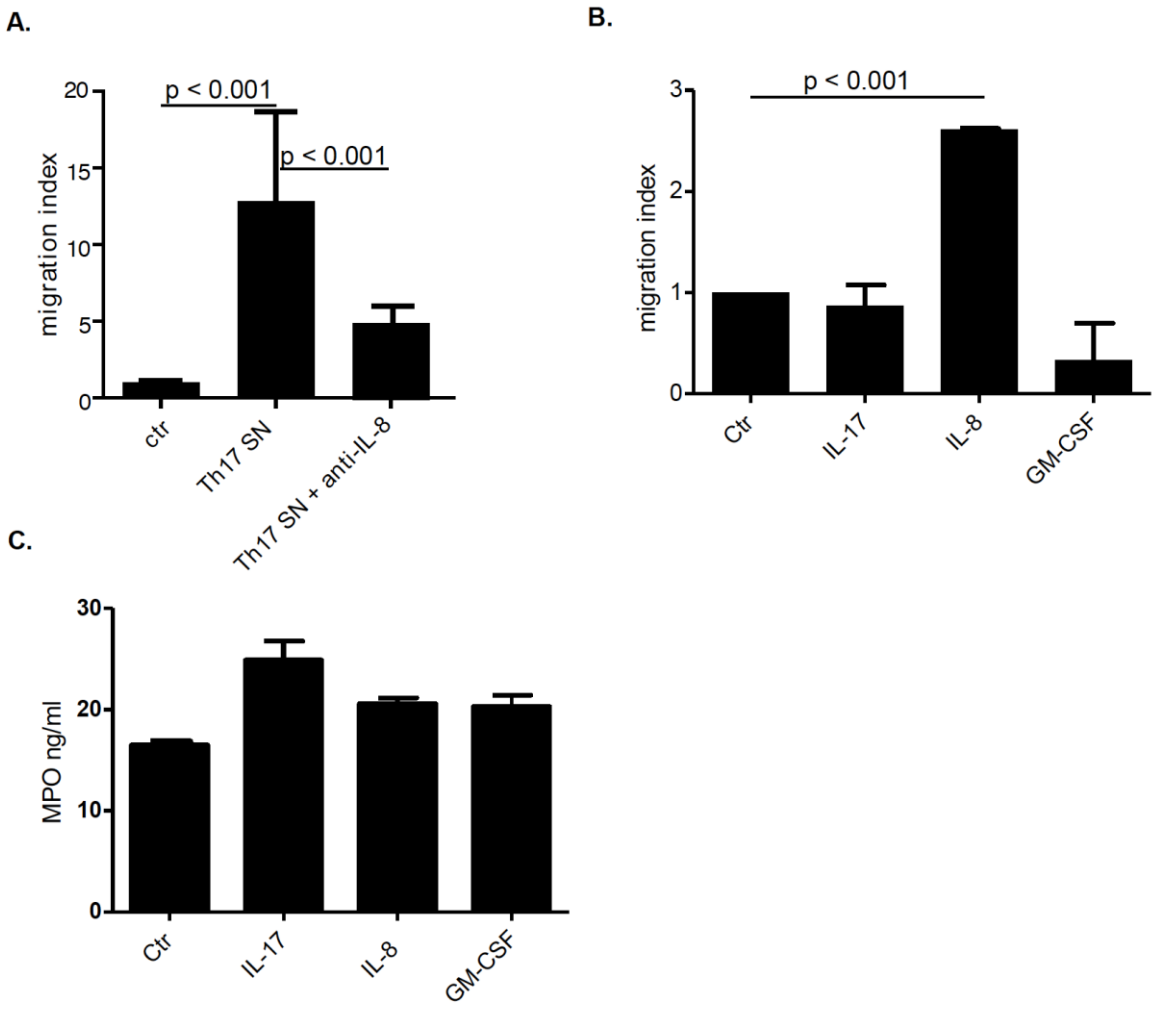

Figure S7. Role of individual Th17-derived cytokines in neutrophil recruitment and activation. A. Migration of neutrophils, purified from blood of healthy donors, towards control medium (Ctr), supernatants from Th17 bulk populations (Th17 SN), or Th17 bulk supernatants pre-treated with anti-IL-8 (Th17 SN+ anti-IL-8). Data refer to experimental triplicates from 3 independent experiments performed with supernatants from bulk populations from 3 different samples. Means ± SD are depicted. Statistical significance was assessed by one-way ANOVA test. **B.** Neutrophil migration in response to recombinant IL-17 (50 ng/ml), IL-8 (100 ng/ml), or GM-CSF (100 ng/ml). Means ± SD of experimental replicates are depicted. **C.** MPO release by neutrophils exposed to control medium (Ctr) or recombinant cytokines, was assessed after a 4-hour incubation by ELISA. Means ± SD of experimental replicates are depicted. Statistical significance was assessed by one-way ANOVA test.

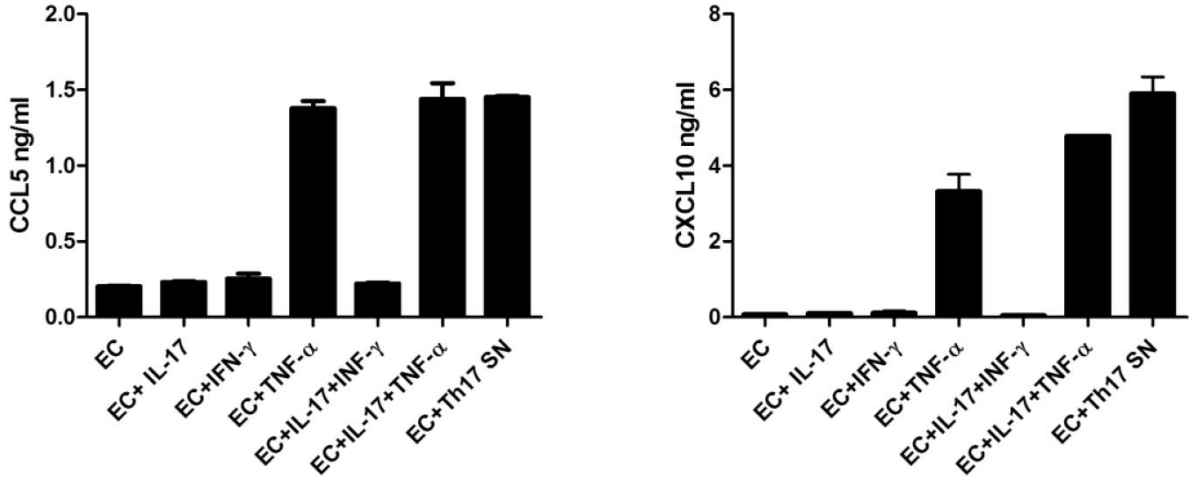

Figure S8. Effects of Th17 cytokines on chemokine release from endothelial cells. Chemokine release by endothelial cells untreated (EC) or exposed to rIL-17 (50 ng/ml) (EC+IL-17), rIFN-γ (1 ng/ml) (EC+IFN-γ), rTNF-α (1 ng/ml) (EC+TNF-α), to the combination of them (EC+IL-17+IFN-γ) (EC+IL-17+TNF-α), or Th17 clone supernatants (EC +Th17 SN) for an overnight period, was measured by ELISA. Means ± SD of experimental triplicates are depicted.

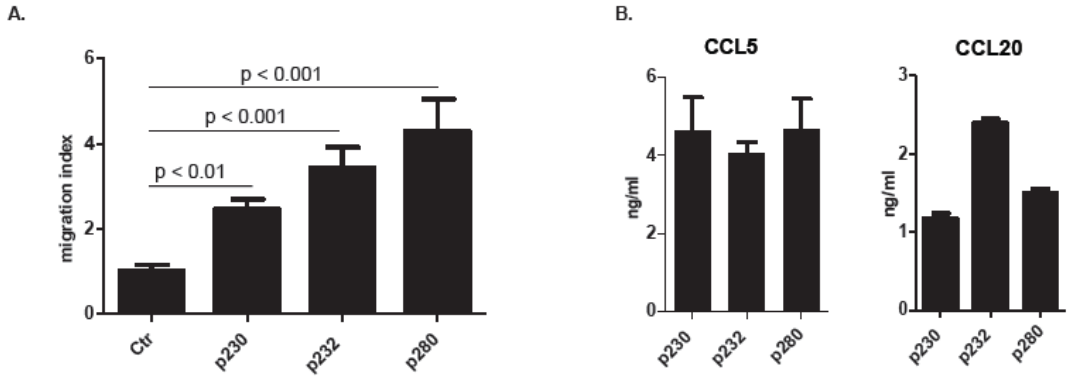

Figure S9. Chemo-attraction of CTLs by Th17 bulk populations. CTL chemo-attraction capacity (**A.**) and chemokine contents (**B.**) of supernatants from Th17 bulk populations expanded from 3 different samples.

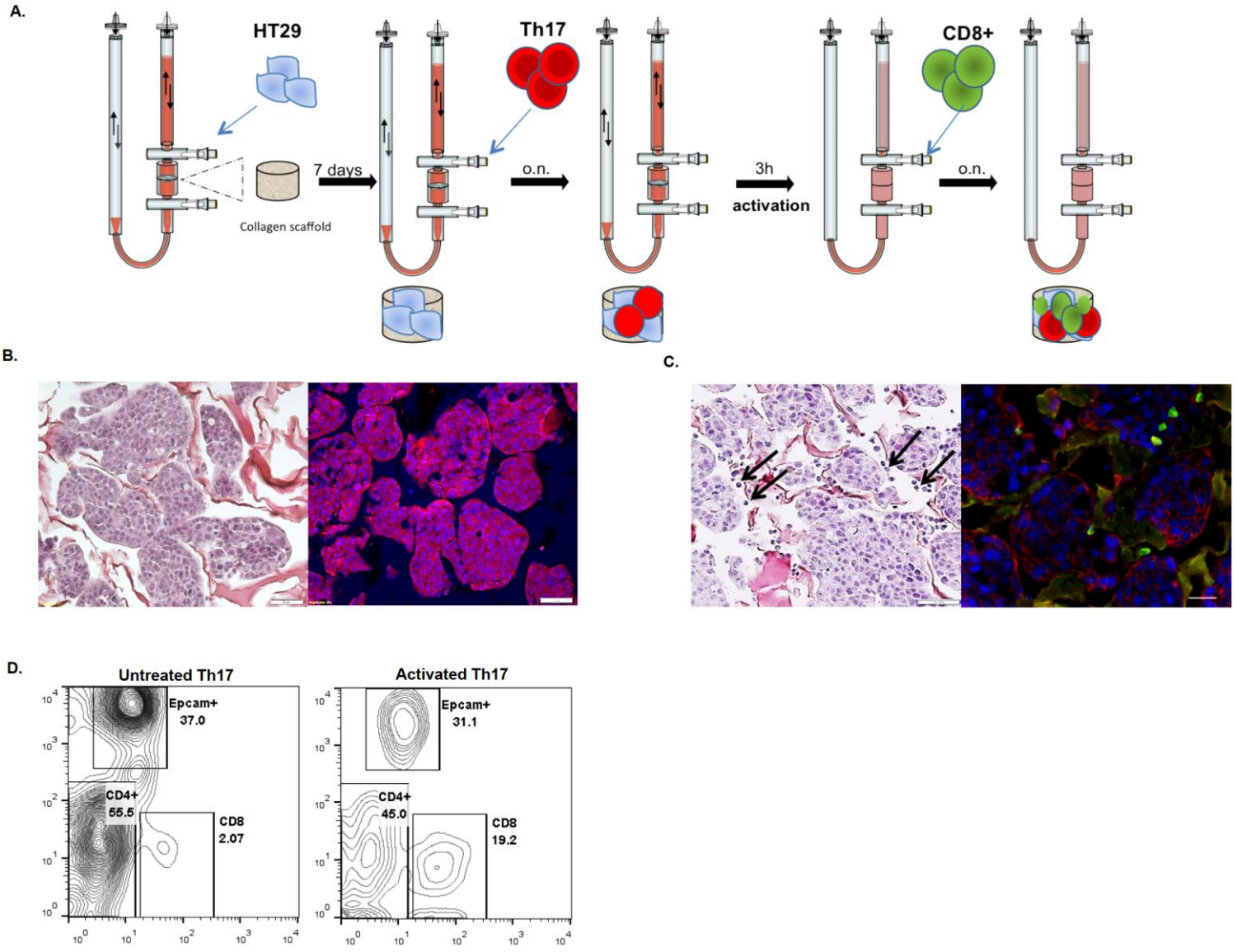

Figure S10: Engineering of tumor-like tissues. A. Experimental protocol: HT29 cells were injected on a collagen scaffold and perfused for 7 days. Th17 cells were then seeded for an overnight period (o.n.) and subsequently activated by adding CytoStim to the perfusion medium. Three hours after Th17 activation, the medium was changed and the system was extensively washed. The perfusion was then stopped, and CD8+ T cells were added into the system. After an overnight incubation the tissue was removed and processed. **B.** H&E staining (left panel) and immunofluorescence analysis (right panel, EpCAM red, DAPI blue) of an engineered tumor tissue at day 7. Scale bar 50 μm. **C.** H&E staining of engineered tumor tissue in the presence of CRC-Th17 (indicated by arrows) and immunofluorescence analysis (right panel, IL-17 green, EpCAM red, DAPI blue). Scale bar 50 μm and 20 μm. **D.** Flow cytometric analysis of single cell suspensions obtained from engineered tumor tissues infiltrated by untreated or activated Th17 cells, upon staining with EpCAM-, CD4- and CD8-specific antibodies. Contour plots of one out of 3 experimental replicates are shown.

Clinico-pathological features		IL-17		P-value
		Median / Mean	Min-Max	
All		2 / 9.8	0 - 184	
Tumor location	Right-sided	3 / 12.6	0 - 200	0.38
	Left-sided	3 / 14.3	0 - 332	
MMR-Status	proficient	2 / 8.7	0 - 184	0.03
	deficient	4 / 16.7	0 - 170	
pT stage	pT1-2	3 / 8.2	0 -80	0.72
	pT3-4	3 / 10.6	0 - 180	
pN stage	pN0	3 / 10.3	0 - 170	0.11
	pN1-2	2 / 10.4	0 - 184	
Tumor grade	G1-2	2 /9.2	0 - 184	0.02
	G3	5 / 17.7	0 – 132	
Vascular invasion	Absent	3 / 9.8	0 – 170	0.42
	Present	2 / 11.8	0 – 184	
Tumor border	Pushing	4 / 11.9	0 – 130	**0.006**
	Infiltrating	2 / 9.1	0 – 184	
Local recurrence	Absent	3 / 8.4	0 – 100	**0.002**
	Present	0 / 4.8	0 – 88	
Distant metastasis	Absent	2 / 7.5	0 - 100	0.02
	Present	0 / 4.6	0 – 34	
Death	Censured	3 / 10.5	0 - 170	0.25
	Present	4 / 13.8	0 – 184	

Table S2: Association of intra-epithelial IL-17+ cells and clinico-pathological features in CRC (n=746)